Ultrasonics Sonochemistry 100 (2023) 106638

Contents lists available at ScienceDirect

Ultrasonics Sonochemistry

journal homepage: www.elsevier.com/locate/ultson

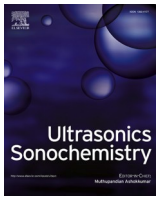

Improvement of the emulsifying properties of *Zanthoxylum* seed protein by ultrasonic modification

Qingqing Liu [a,b,*], Yanting Liu [a,b], He Huang [a,b], Mingming Xiong [a,b], Yunting Yang [a,b], Chutian Lin [a,b], Feng Yang [a,b], Yisha Xie [a,b], Yongjun Yuan [a,b,*]

[a] Chongqing Key Laboratory of Speciality Food Co-Built by Sichuan and Chongqing, School of Food and Bioengineering, Xihua University, Chengdu 610039, China
[b] Key Laboratory of Grain and Oil Processing and Food Safety of Sichuan Province, College of Food and Bioengineering, Xihua University, Chengdu 610039, China

ARTICLE INFO

Keywords:
Zanthoxylum seed protein
Ultrasonic treatment
Protein structure
Emulsifying properties

ABSTRACT

The influence of ultrasonic treatment (100–500 W, 30 min) on the molecular structures and emulsifying properties of *Zanthoxylum* seed protein (ZSP) was explored for the first time in this work. Research results indicated that the all ultrasonic treatments at different power levels decreased the particle size but increased the surface charge of ZSP. In addition, the ultrasonic treatments induced the structural unfolding of the ZAP, as indicated by the increase in α-helix, ultraviolet–visible absorbance, surface hydrophobicity and the amount of surface free sulfhydryl groups, as well as the decrease in β-sheet and intrinsic fluorescence intensity. As a result, the significantly ($p < 0.05$) increased emulsifying activity index (EAI) and emulsion stability index (ESI) of ZSP were observed after ultrasonic treatment. In addition, the emulsion prepared by ultrasonically treated ZSP exhibited the smaller and more uniform droplets with significantly improved stability against environmental stress (temperature, salt concentration, pH), creaming and oxidation due to the increased ratio of interfacially adsorbed ZSP. Furthermore, ultrasonic treatment at 400 W was found to be the optimum condition for modification. These findings will provide a theoretical foundation for the utilization of ultrasound in enhancing the emulsifying properties of ZSP and promoting its application in the field of food processing.

1. Introduction

In recent years, the demand for food, particularly protein, has increased due to continued global population growth [1]. In addition, vegetable proteins have been increasingly considered as alternatives to animal proteins to meet human health and nutritional requirements due to their high nutritional value, low cost and environmental friendliness [2,3]. Although soy protein has been widely used in the food industry, the ingestion of soy protein might lead to severe allergic responses (e.g. anaphylactic shock) due to the presence of allergens (β-conglycinin, glycinin and others) [4]. Meanwhile, there are some anti-nutritional factors (phytates and others) in soy protein, limiting its digestion [5]. Therefore, more plant proteins still need to be developed. In particular, the utilization of by-products from plant food processing for protein extraction presents a viable and eco-friendly solution that minimizes resource wastage and mitigates environmental pollution [3]. The seeds of *Zanthoxylum bungeanum* seeds, which account for approximately 60 % of the total weight of *Zanthoxylum bungeanum*, are rarely used and are considered to be the main by-products of its processing, while only the s are widely used for the production of food seasoning or essential oil [6]. *Zanthoxylum bungeanum* seeds contain about 18 %–20 % protein, which contains 17 types of amino acids and has some biological activity (e.g., antibacterial activity, nerve-blocking activity) after digestion, meanwhile, *Zanthoxylum bungeanum* seeds have not been found to contain any toxic substances, anti-nutritional factors or allergens [6]. As the annual production of *Zanthoxylum* is over 500,000 tonnes [7], the amount of discarded seeds is over 300,000 tones. It is therefore necessary to make full use of ZSP to increase the value of *Zanthoxylum* seeds.

Emulsions, particularly those of the oil-in-water (O/W) type, are frequently present in a variety of food products like condiments, sweets, and drinks. Proteins are extensively utilized as emulsifying agents in these systems owing to their rich nutritional content and favorable functional attributes [8]. Thus, the emulsifying properties of proteins, as one of their most important functional properties, have attracted much

* Corresponding authors at: Chongqing Key Laboratory of Speciality Food Co-Built by Sichuan and Chongqing, School of Food and Bioengineering, Xihua University, Chengdu 610039, China.
E-mail addresses: liuqing_861006@163.com (Q. Liu), yyja9791@sina.com (Y. Yuan).

https://doi.org/10.1016/j.ultsonch.2023.106638
Received 12 July 2023; Received in revised form 20 September 2023; Accepted 6 October 2023
Available online 7 October 2023

attention from researchers. However, native proteins are generally unable to rapidly adsorb, unfold and rearrange at the oil/water interface to form a strong viscoelastic film due to their inappropriate surface hydrophobicity/hydrophilicity, poor flexibility and high sensitivity to ambient conditions (e.g., temperature, salt concentration, pH and others), leading to emulsion destabilization [9]. The poor emulsifying properties of *Zanthoxylum* seed protein (ZSP) have been previously demonstrated [10] and confirmed through our preliminary experiment. It is therefore necessary to investigate an appropriate approach to improve the emulsifying properties of ZSP. However, there is no report about this so far.

Ultrasonic treatment, especially low frequency ultrasonic treatment (10–60 kHz), has been commonly applied to improve the emulsifying properties of various food proteins, e.g., walnut protein [11], wheat germ protein [2], *Neosalanx taihuensis* myofibrillar protein [12], perilla protein isolate [3] and others. Ultrasonic modification of protein is commonly attributed to the alteration in protein structure caused by the effects of acoustic cavitation produced by ultrasound, along with its resulting physical, chemical, and thermal impacts. The physical consequences encompass intense mechanical shear forces, elevated pressure levels, shock waves, microjets, turbulence and acoustic flow. The chemical outcomes involve the disruption of covalent bonds within water molecules that lead to the generation of H•, •OH radicals and even H_2O_2 [9]. Based on the literature reports, we postulate that high-intensity ultrasound will exert a positive impact on the structural modifications and emulsifying properties of ZAP, thereby enhancing the stability of the emulsion. However, this phenomenon remains unreported.

Thus, in order to confirm our hypothesis, ZSP was subjected to ultrasonic treatment (100–500 W, 30 min) and characterized by the molecular weight, particle size, zeta-potential and secondary/tertiary structure. In addition, the emulsifying properties were appraised by measuring the emulsifying activity/stability index (EAI/ESI). Furthermore, the characters (e.g., the interfacial protein adsorption, microstructure, particle size, zeta-potential, static rheological behaviour) and stabilities (e.g., creaming stability, and oxidative stability) of the emulsions were characterized. This research may offer a fundamental basis for enhancing the emulsifying properties of ZSP through ultrasonic modification and extending its utilization in food industry.

2. Materials and methods

2.1. Materials

ZBM seed and soybean oil (containing *tert*-butylhydroquinone (TBHQ) as the only antioxidant) was acquired from a local market (Chengdu, China). Sodium dodecyl sulfate (SDS), glycerol, acrylamide, N, N′-methylene-bis-acrylamide, Bromophenol blue sodium salt, Coomassie Brilliant Blue R-250, β-mercaptoethanol, Potassium bromide (KBr), 8-Anilino-1-naphthalenesulfonic acid (ANS), 5,5′-dithio-bis-nitrobenzoic acid (DTNB), cumene hydroperoxide, 1,1,3,3-tetraethoxypropane, Coomassie Brilliant Blue G-250 and bovine serum albumin (BSA), were procured from the Aladdin Reagent Co. (Shanghai, China). Sodium azide were procured from Sigma-Aldrich (Shanghai, China). Other chemical reagents (e.g., petroleum ether, hydrochloric acid (HCl), sodium hydroxide (NaOH), acetic acid, sodium dihydrogen phosphate (NaH2PO4), disodium hydrogen phosphate (Na2HPO4), Tris (hydroxymethyl) aminomethane (Tris), ethanol, 2-propanol, isooctane, 1-butanol, methanol, ammonium thiocyanate, ferrous sulfate (FeSO4), barium chloride ($BaCl_2$), thiobarbituric acid (TBA), trichloroacetic acid (TCA) and others) were analytical pure and procured from Cologne Chemical Co. (Chengdu, China).

2.2. Preparation of ZSP

ZSP was isolated following the previously reported procedure with minor modifications [6]. After removal of foreign matter, *Zanthoxylum bungeanum* seeds were washed, dried and ground to produce a fine powder (100 mesh) and then defatted with petroleum ether (1:5, w/v) with gentle stirring at room temperature for 2 h. Centrifugation (2656 g, 4 °C, 15 min) was used to remove the petroleum ether. The defatting procedure was repeated three times until the crude fat content did not exceed 0.5 % [13]. The defatted *Zanthoxylum bungeanum* seed powder was then dispersed in sodium hydroxide (NaOH) solution (pH 10.0, 1:20, w/v). After stirring for 40 min (40 °C, 500 rpm) and centrifugation (1574 g, 4 °C, 20 min), the pH of the supernatant was adjusted to 4.5 with 1 M HCl. Finally, ZSP was precipitated by centrifugation (10,000 *g*, 4 °C, 30 min), redispersed in distilled water (the pH was adjusted to neutral), dialyzed with distilled water (48 h) to remove salt. The resulting ZSP solution was dried in a freeze-dryer (SCIENTZ-10ND, Ningbo Scientz Biotechnology Co. Ltd, China) for approximately 48 h. The ZSP powders were placed into a ziplock bag and stored at −20 °C.

2.3. Ultrasonic treatment of ZSP

100 mL of ZSP dispersions (2 %, w/v) were prepared with distilled water and modified using an ultrasonic device (JY92-2D, Ningbo Scientz Biotechnology Co. Ltd, China) equipped with a titanium probe (diameter of 0.636 cm) at 100–500 W for 30 min (2 s on, 2 s off) [14]. The temperature was controlled at 25 °C during sonication. Finally, all ultrasonically treated protein samples were lyophilized and then reserved at −20 °C.

2.4. Molecular weight distribution

Sodium dodecyl sulfate–polyacrylamide gel electrophoresis (SDS-PAGE) was applied to analyze the molecular weight distribution of the protein samples [15]. The acrylamide solution with a concentration of 5 % and 12 % was utilized for the preparation of stacking gel and the resolving gel, respectively. Tris-HCl buffer solution (0.124 M, pH 6.8) containing 15 % of glycerol (v/v) and 2 % of SDS (w/v) was used as the sample loading buffer. For reducing conditions, β-mercaptoethanol (5 %, v/v) was added. The molecular mass standard contained proteins with different sizes (14.4, 18.4, 25, 35, 45, 66.2 and 116 kDa). The electrophoretic analysis was conducted using a Bio-Rad Mini-PROTEAN II System Cell apparatus (Bio-Rad Laboratories Inc., Hercules, CA, USA) at a constant voltage of 120 V for an hour. The gel was stained with 0.1 % Coomassie Brilliant Blue R-250 for 15 min, and then decolored with methanol-acetic acid–water ternary buffer (50:100:850) for 3 times.

2.5. Particle size and zeta-potential

The protein powder was dissolved in phosphate buffer solution (pH 7.0, 10 mmol/L) at 1.0 mg/mL. A Zetasizer Nano-ZS 90 (Malvern Instruments, Malvern, UK) was applied to determine the particle size distribution, mean particle size and zeta-potential of the protein solutions at room temperature [16]. Each sample underwent three measurements, and the resulting data were documented as the mean ± standard deviation.

2.6. Secondary structure

The infrared spectra of ZSP were measured using a Fourier transform infrared spectrophotometer (Nicolet iS10, ThermoFisher scientific, USA). KBr was dried at 105 ℃ to a balanced weight. Protein sample and KBr were blended in an agate mortar (1:49, w/w) and ground. The ground powder was then placed in a tablet press and pressed into transparent flakes. Spectral data were obtained in the wave number range of 400–4000 cm^{-1} by 32 scans and 1 cm^{-1} resolution. Protein secondary structure was analyzed by deconvolution and second derivation of the amide I band (1600–1700 cm^{-1}) using Omnic 9 software (ThermoFisher scientific, America) [17]. Each sample underwent three

measurements, and the resulting data were documented as the mean ± standard deviation.

2.7. Tertiary structures

2.7.1. Ultraviolet–visible (UV–Vis) spectrum

The protein powder was dissolved in phosphate buffer solution (pH 7.0, 10 mmol/L) at 1.0 mg/mL and analyzed using a UV–vis spectrophotometer (SDPTOP UV-2400, Shanghai, China) at a wavelength of 200–700 nm. The measurement was performed at 25 °C with phosphate buffer solution as a blank [18].

2.7.2. Intrinsic fluorescence spectrum

The protein sample was solubilized in distilled water at 0.2 mg/mL and analyzed by a Fluoromax-4 spectrofluorometer (Horiba Scientific, USA) at 20 °C. The excitation wavelength was set to 290 nm and the fluorescence intensity was measured at 310–500 nm (emission) [14]. The slit width and the scanning speed were 5.0 nm and 5 nm/s, respectively.

2.7.3. Surface hydrophobicity

ZSP solutions with different concentration (0.025 to 0.2 mg/mL) were prepared. Then, 0.02 mL phosphate buffer solution (pH 7.0, 10 mmol/L) containing 8 mM ANS was combined with 4 mL of the respective protein solutions and maintained for 15 min. A Fluoromax-4 spectrofluorometer (Horiba Scientific, USA) was employed to measure the relative fluorescence intensity at 470 nm (emission). The excitation wavelength was set at 390 nm. The surface hydrophobicity was calculated by the initial slope factor of the fluorescence intensity versus protein concentration [14]. Each sample underwent three measurements, and the resulting data were documented as the mean ± standard deviation.

2.7.4. Surface free sulfhydryl (SH) content

Surface free SH groups in proteins were counted followed by a previous method [19]. Briefly, protein solution (5 mg/mL) and DTNB (4 mg/mL) solution were respectively prepared with Tris-HCl buffer (pH 8.0), mixed (100:1, V/V) and incubated (25 °C, 15 min). The supernatant was then collected after centrifugation (8000 *g*, 10 min) and measured by a spectrophotometer (SDPTOP UV-2400, Shanghai, China) at 412 nm. The molar extinction coefficient to count the amount of SH groups is 13600 M^{-1} cm^{-1}. Each sample underwent three measurements, and the resulting data were documented as the mean ± standard deviation.

2.8. Preparation of emulsion

The TBHQ in the soybean oil was completely removed by ethanol following to the previously reported method [20] to eliminate its influence on the oxidative stability of the emulsions. After that, native or ultrasonically treated ZSP dispersions (10 mg/mL) were prepared and blended with soybean oil (3:1, V/V). Each mixture was homogenized (13,500 rpm, 2 min) using a high-speed homogenizer (T25, IKA, Germany) and subsequently homogenized (30 MPa, twice) using a high-pressure homogenizer (Scientz-150, Ningbo Scientz Biotechnology Co. Ltd, China) to form emulsion [21,22]. Sodium azide was mixed with the emulsion (0.02 %, w/v) to prevent microbial growth. The emulsions were analyzed promptly after preparation, except for the determination of creaming stability and oxidative stability [8].

2.9. EAI and ESI

EAI and ESI were determined using a previously reported method [23] with minor modifications. Briefly, 0.02 mL of emulsion (formulated in section 2.8) was collected from the bottom of the beaker at 0/30 min, and then diluted with 4.98 mL of SDS solution (0.1 %, w/w). The optical density at 500 nm was determined (SDPTOP UV-2400, Shanghai, China) using SDS solution as a blank (optical path of 1.0 cm). The formulae for the calculation of the EAI and ESI are:

$$EAI\left(m^2/g\right) = (2 \times 2.303 \times A_0 \times N)/[c \times (1-\phi) \times 10^4] \quad (1)$$

$$ESI(\text{min}) = 30 \times A_0/(A_0 - A_{30}) \quad (2)$$

In these two equations, A_0/A_{30} is the optical density of the diluted emulsion at 0/30 min, N denotes the dilution multiple (250), c is the protein concentration of the ZSP solution (0.01 g/mL), Φ represents the volume fraction of the oil in the emulsion (0.25). Each emulsion underwent three measurements, and the resulting data were documented as the mean ± standard deviation.

2.10. Droplet size and zeta-potential of emulsion

A Zetasizer Nano-ZS 90 (Malvern Instruments, Malvern, UK) was used to examine the droplet size dispersion, mean droplet size and zeta-potential of the emulsions formulated in section 2.8 [24]. Briefly, each emulsion was diluted for 500-fold with phosphate buffer solution (pH 7.0, 10 mmol/L) and subsequently measured by dynamic light scattering. Each emulsion underwent three measurements, and the resulting data were documented as the mean ± standard deviation.

2.11. Microstructure of the emulsion

An optical microscope (Nikon Eclipse E200, Tokyo, Japan) was applied to obtain the microstructure of the emulsions formulated in section 2.8.

2.12. The interfacial protein adsorption of emulsion

The emulsions (formulated in section 2.8) were centrifuged (10,000 *g*, 15 min) to separate them into two layers. The upper and lower layers were the emulsified and aqueous layers, respectively. A syringe was used to separate the aqueous layer and the protein content was determined by the Coomassie Brilliant Blue G-250 method [25]. The formula for calculating the interfacial adsorbed protein ratio of the fine emulsion is as follows:

$$Interfacial\ adsorbed\ protein(\%) = [(C_0 - C_l)/C_0] \times 100 \quad (3)$$

where C_0 and C_l represent protein content in the whole emulsion systems and the aqueous layer (after centrifugation), respectively. Each emulsion underwent three measurements, and the resulting data were documented as the mean ± standard deviation.

2.13. Static rheological measurement

The rheological behaviour of the emulsions was measured at 25 °C using a rotational rheometer (MCR-301, Anton Paar, Austria) equipped with a parallel plate (60 mm diameter and 1 mm gap). The shear rate was set from 0.1 s^{-1} to 100 s^{-1} [26].

2.14. The stability of emulsions against environmental stresses

The fresh emulsion (3 mL) was placed into a glass tube and underwent a series of different procedures. Initially, it underwent a 30 min duration of heating in a water bath at temperatures ranging from 70 to 90 ℃. Subsequently, an addition of NaCl solution (0.3 mL) with concentrations ranging from 100 to 300 mM was performed, followed by storage of the emulsion at a temperature of 25 ℃ for two hours. Thirdly, the pH level of the emulsion was adjusted to values of 3, 5, 7 and 9 using 0.1 M NaOH/HCl, thereafter, the emulsion was kept for 2 h at 25℃. Finally, the particle size of the treated emulsions was determined by employing the procedure outlined in section 2.10. Each emulsion

underwent three measurements, and the resulting data were documented as the mean ± standard deviation.

2.15. Creaming index of emulsion

The emulsions that were formulated in section 2.8 were moved into glass bottles and sealed. The height of the whole emulsion systems and the aqueous layer was assessed at 0–7 d, respectively [27]. The creaming index was calculated as follows:

$$Creaming\ index(\%) = (H_a/H_t) \times 100 \quad (4)$$

In this equation, H_a and H_t represent the height of the aqueous layer and the whole emulsion system, respectively. Each emulsion underwent three measurements, and the resulting data were documented as the mean ± standard deviation.

2.16. Oxidative induction measurement

The emulsions that were formulated in section 2.8 were stored at 37 ℃ without illumination to accelerate oxidation [20]. Lipid hydroperoxides and 2-thiobarbituric acid reactive substances (TBARS), corresponding to the primary and secondary products during lipid oxidation, were used to estimate the degree of lipid oxidation following a previous reference. For lipid hydroperoxides analysis, each emulsion sample (0.3 mL) was combined with a mixture of isooctane and 2-propanol (1.5 mL, 3:1, v/v). After vortexed for 30 s, the mixture was centrifuged (1000 rpm, 2 min) to obtain the supernatant. Following this, 200 μL of supernatant was combined with 2.8 mL of methanol-1-butanol mixture (2:1, v/v). To this mixture, ammonium thiocyanate solution (15 μL, 3.94 mol/L) and ferrous solution (15 μL, containing 0.132 mol/L $BaCl_2$ and 0.144 mol/L $FeSO_4$) were added. The resulting mixture was stored at 25 ℃ for 20 min before determining its absorbance at 510 nm using an ultraviolet–visible spectrophotometer (SDPTOP UV-2400, Shanghai, China). A standard curve of cumene hydroperoxide was employed to determine the final hydroperoxide level present in each sample. For TBARS analysis, equal volumes of the emulsion (0.5 mL each) were combined with the TBA reagent (dissolved 15 % TCA and 0.375 % TBA in 0.25 M HCl and boiling for 30 min) and then centrifugated (2,000 g, 10 min). The absorbance of supernatant was measured at 532 nm using an ultraviolet–visible spectrophotometer (SDPTOP UV-2400, Shanghai, China). Calculations of TBARS value were performed utilizing the standard curve of 1,1,3,3-tetraethoxypropane [28]. Each emulsion underwent three measurements, and the resulting data were documented as the mean ± standard deviation.

In addition, the oxidation stability of the emulsion was also measured by the conductivity changes of the emulsion using the 743 Rancimat (Metrohm Co., Switzerland) with 3.0 g of emulsion is heated to 100 ℃ in an air flow of 10 L/h [29]. Each emulsion underwent three measurements, and the resulting data were documented as the mean ± standard deviation.

2.17. Statistical analysis

All the aforementioned measurements were conducted in triplicate and the corresponding data were documented as the mean ± standard deviation. Statistical differences between samples were analysed using SPSS software, with One-way analysis of variance (ANOVA) and Tukey's test ($P < 0.05$).

3. Results and discussion

3.1. SDS-PAGE

SDS-PAGE is commonly applied for the determination of protein molecular weight distribution [3]. Fig. 1 displays the electrophoretic images of ZSP before and after ultrasonic treatment. The difference between the same protein sample in the reducing and non-reducing SDS-PAGE indicated that the presence of disulfide bonds that were broken by β-mercaptoethanol, leading to the generation of smaller subunits [11]. In both the reducing and non-reducing environments, the SDS-PAGE images showed no obvious difference between the native and ultrasonicated ZSP at 100–500 W, suggesting that ultrasonic treatment at 100–500 W induced any no obvious changes in the molecular weight of ZSP [3]. The similar result of SDS-PAGE analysis of the native and ultrasonicated proteins, such as grass pea protein isolate [30], walnut protein [11] have also been reported.

3.2. Particle diameter and zeta-potential

The particle diameter of the protein is essential to reflect its dispersion or aggregation state, and the small size of the protein is advantageous for the formation and stabilization of emulsions [31]. As shown in Fig. 2A and Fig. 2B, native ZSP was unimodally but broadly distributed with a mean particle size of 762.82 ± 6.95 nm, indicating the presence

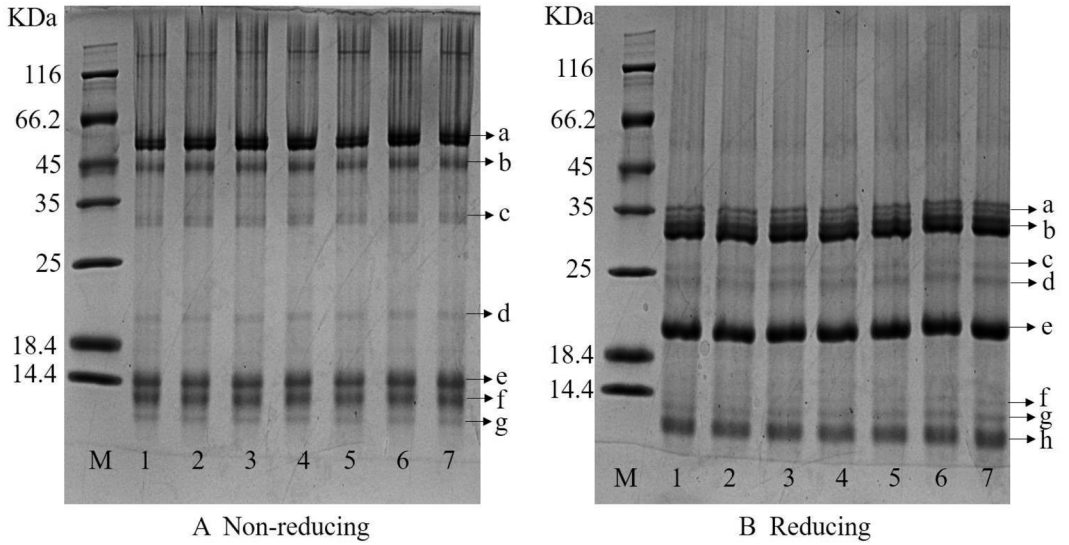

Fig. 1. SDS-PAGE images of native and ultrasonicated ZSP in non-reducing (A) and reducing environments (B). Lane M: marker; lane 1: native ZSP; lane 2–5: ultrasonicated ZSP (100–500 W).

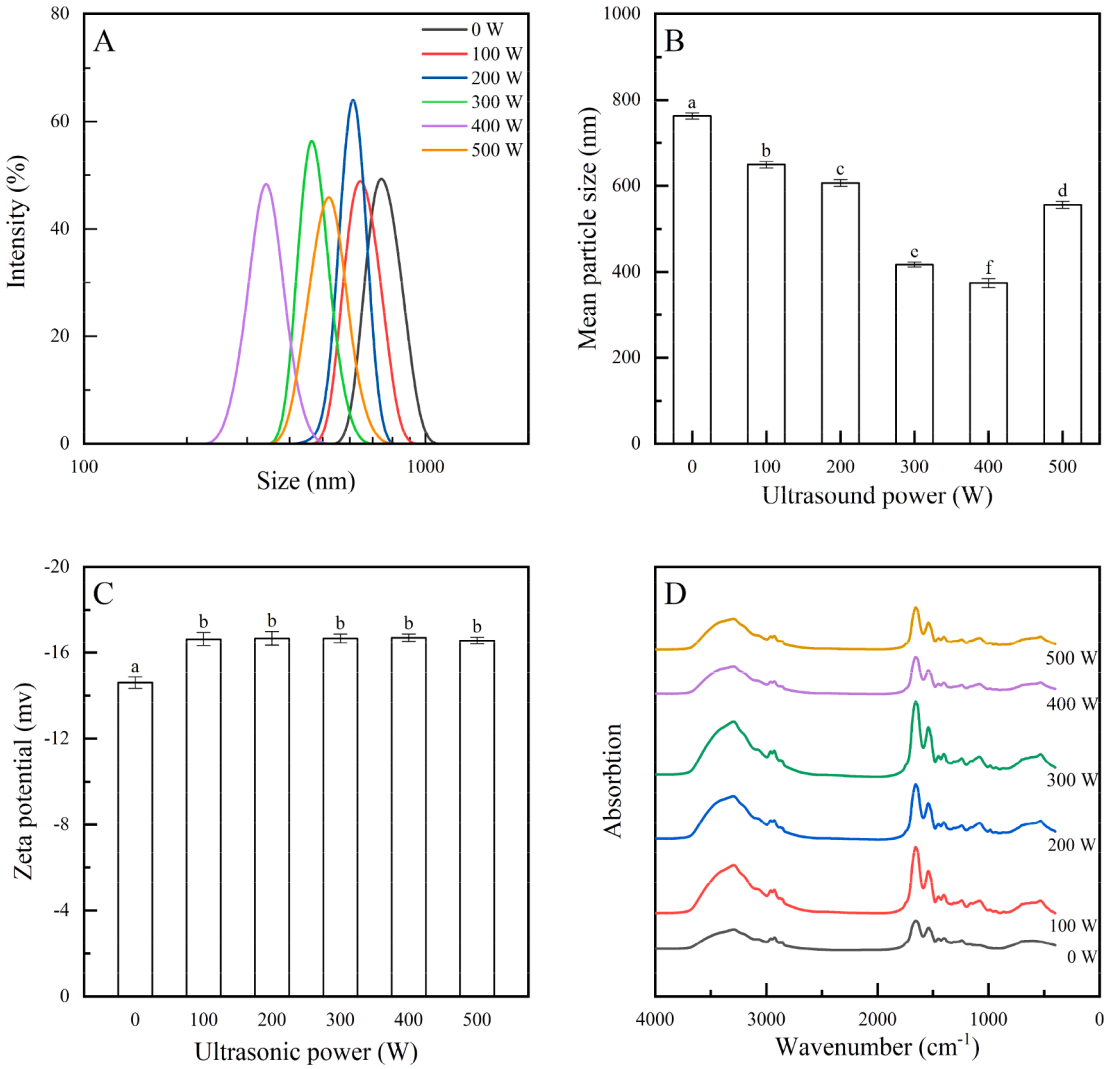

Fig. 2. The particle size dispersion (A), mean particle size (B), zeta-potential (C) and infrared spectra (D) of native and ultrasonicated ZSP. Different lowercase letters in the column diagram suggest significant differences ($P < 0.05$).

of large aggregates in the ZSP sample. The large protein aggregates have also been observed in other plant protein isolates such as faba bean protein [32], quinoa protein [33] and others, which are thought to be formed by intermolecular aggregation during protein extraction processes [32]. After ultrasonication at 100–400 W, the particle size dispersion curve of ZSP was gradually narrowed and moved to the smaller size, with the mean size of ZSP also gradually decreasing and reaching the minimum value (373.86 ± 10.89 nm) at 400 W. The decreased particle size of ZSP can be ascribed to the breaking of the chemical bonds of proteins (e.g., electrostatic interactions, hydrogen bonding and others) by the cavitation, high hydrodynamic shear force and micro-streaming generated during ultrasonication [3,32]. The reduced particle diameter after ultrasonication was also reported in quinoa protein [33]. However, the mean particle size of ZSP increased as the ultrasonic power was further increased, similar to the previous reports [8], which could be attributed to the excessive protein denaturation and reaggregation of dissociated proteins at the excessive ultrasonic power.

Zeta potential serves as an indicator of the overall surface charges of particles, providing insights into the aggregation and stability of particles in in solution and emulsion [3,8]. As shown in Fig. 2C, all ZSP samples displayed negative zeta-potential at neutral pH, suggesting an abundance of negatively charged amino acids compared to positively charged ones on the surface of ZSP. In addition, a minor rise in the negative zeta-potential of ZSP was observed after ultrasonic treatment at 100–500 W, which could be due to the depolymerization of ZSP, increasing the surface exposure of negatively charged amino acids [14]. The stability of the protein solution increases with a higher zeta-potential due to the enhanced repulsive force between particles, resulting in reduced aggregation tendency [8]. In addition, the zeta-potential of the protein is also important for the stability of emulsion, as the charged proteins interfacially adsorbed could charge the emulsion droplets and increase electrostatic repulsion, preventing the droplet collisions and contributing to the emulsion stability [8]. Similar increases in negative charge have been observed after ultrasonic treatment of *Cyperus esculentus* seed (tiger nut) protein [14], grass pea protein isolate [30] and others.

3.3. Secondary structure

Protein secondary structures are strongly correlated to their emulsifying properties [24]. As shown in Fig. 2D and Table 1, the proportions of α-helix, β-sheet, β-turn and random coil of native ZSP were 20.19 ± 0.32 %, 34.39 ± 0.38 %, 25.84 ± 0.26 % and 19.58 ± 0.28 %, respectively. After ultrasonic treatment at 100–500 W, the proportions of α-helix were gradually increased, while the percentages of β-turn and β-sheet were gradually decreased, probably due to the vibration, collision and rearrangement of ZSP molecules during ultrasonication [33].

Table 1
Secondary structure of native and ultrasonicated ZSP.

Ultrasonicpower (W)	Secondary structure content (%)			
	α-helix	β-sheet	β-turn	Random coil
0	20.19 ± 0.32[a]	34.39 ± 0.38[b]	25.84 ± 0.26[b]	19.58 ± 0.28[a]
100	22.81 ± 0.46[b]	32.42 ± 0.33[a]	24.71 ± 0.34[a]	19.26 ± 0.37[a]
200	23.06 ± 0.63[b]	32.55 ± 0.42[a]	24.65 ± 0.33[a]	19.19 ± 0.62[a]
300	22.82 ± 0.37[b]	32.32 ± 0.34[a]	24.69 ± 0.36[a]	19.37 ± 0.21[a]
400	23.25 ± 0.43[b]	32.53 ± 0.56[a]	24.54 ± 0.54[a]	19.68 ± 0.59[a]
500	23.21 ± 0.59[b]	32.47 ± 0.29[a]	24.61 ± 0.32[a]	19.71 ± 0.35[a]

[a] The spectral regions of 1692–1662 cm^{-1}, 1662–1645 cm^{-1}, and 1645–1638 cm^{-1} are the β-turn, α-helix, and random coil structures, respectively, and the regions of 1692–1700 cm^{-1} and 1615–1638 cm^{-1} are the β-sheet structure [42].
[b] Different lowercase letters in each column suggest significant differences ($p < 0.05$).

Similar increases in the proportion of α-helix content and decreases in the proportion of β-sheet have also been observed after ultrasonic treatment of perilla protein isolate, quinoa protein and wheat germ protein [2,3,33]. In general, the α-helix is the most compact structure of proteins. The increased proportion of α-helix means the more compact structure of protein molecules, which was helpful to keep the structural integrity of proteins throughout emulsion formation and storage [3,33]. However, the opposite trend of secondary structure change has been observed for cactus (*Opuntia ficus-indica*) seed protein [13], grass pea (*Lathyrus sativus L.*) protein [30] and others. These differences can be due to the differences in protein types, major secondary structure types, denaturation levels, aggregation states, ultrasound conditions and others [3].

3.4. Tertiary conformations of ZSP

3.4.1. UV–vis absorption spectroscopy

UV–vis absorption spectroscopy is an effective method for assessing the microenvironmental variation of aromatic amino acid residues (tyrosine, phenylalanine and tryptophan), which reflects the tertiary structure variation of proteins [3,18,30]. As depicted in Fig. 3A, an absorption peak occurred at around 276 nm for both native and ultrasonicated ZSP. The absorption of the ZSP also increased with the ultrasonic power increasing from 100 W to 400 W, reaching a maximum value at 400 W. A similar increase in UV–vis absorption has also been reported for perilla protein isolate and grass pea (*Lathyrus sativus L.*) protein isolate [3,30], which could be due to the partial unfolding of the

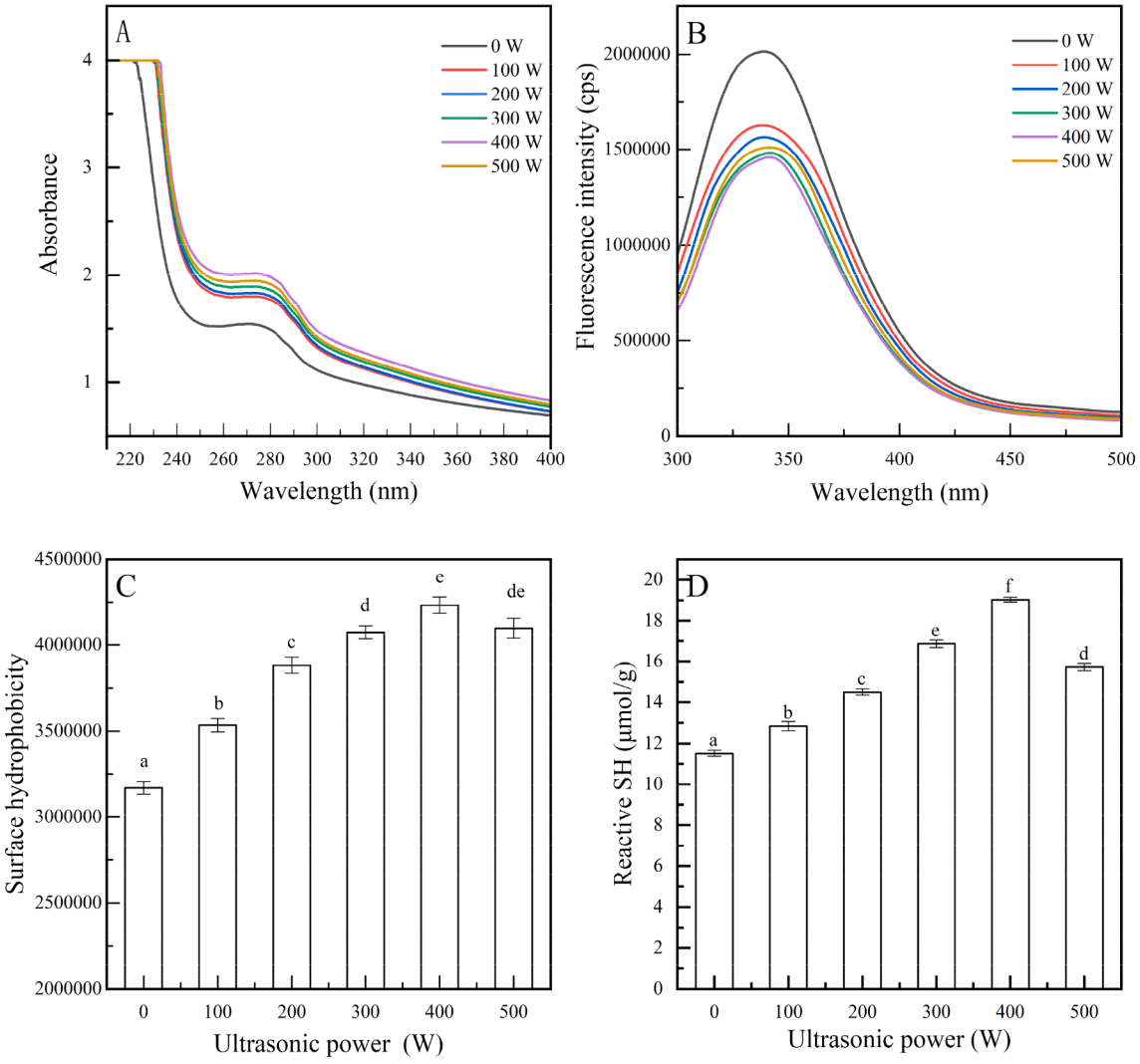

Fig. 3. UV–vis spectrum (A), intrinsic fluorescence spectrum (B), surface hydrophobicity (C) and surface SH (D) of native and ultrasonicated ZSP. Different lowercase letters in column diagram suggest significant differences ($P < 0.05$).

proteins induced by the ultrasonic treatment, increasing the surface exposure of hydrophobic groups (e.g. tyrosine, phenylalanine and tryptophan) [3,18,30]. On the other hand, a slight decrease in UV–vis absorption was observed with further increase in the ultrasonic power, consistent with the report of Zhao et al. and Yan et al. [3,8], which probably due to the extensive protein denaturation and reaggregation at excessive power, reburying the exposed hydrophobic groups [3]. Another possible reason for the reduced absorption intensity at the excessive ultrasound power could be due to the generation of hydrogen peroxide as a result of water sonolysis under strong cavitation, leading to the oxidation of these aromatic amino acid residues [9,30].

3.4.2. Intrinsic fluorescence spectra analysis

Intrinsic fluorescence spectrum, mainly derived from the aromatic amino acid residues, are also a traditional approach to assess the tertiary structure variation of proteins [3]. As shown in Fig. 3B, the maximum fluorescence intensity (λmax) of native ZSP was 338 nm. After ultrasonication at 100–400 W, the λmax of ZSP gradually moved to the higher wavelength, indicating that the aromatic amino acid residues, especially tryptophan residues, migrated to the protein surface and increased their microenvironmental hydrophilicity [3]. In addition, the maximum fluorescence intensity was observed in native ZSP and significantly decreased after ultrasonic treatment at 100–400 W, which can be attributed to the ultrasound-induced conformational transformation of ZSP, exposing more chromophore to the solvent, as well as the oxidation of tryptophan residues [3]. Similar increases in λmax and decreases in fluorescence intensity have also been reported for perilla protein isolate, Tenebrio molitor protein and others [3,31]. However, the fluorescence intensity increased slightly with further increase in ultrasonic power, consistent with the report of Zhao et al. and Yan et al. [3,8], suggesting that some of the exposed chromophore would be reburied at excessive ultrasonic power due to the structural change of protein. In addition, the increased particle size of the ultrasonicated ZSP at 500 W would also contribute to the rebury of the exposed chromophore and lead to the higher fluorescence intensity.

3.4.3. Surface hydrophobicity of ZSP

The amount of hydrophobic group on the surface of proteins is defined as surface hydrophobicity, which reflects the tertiary structure variation of proteins and is critical to their emulsifying properties [2,30]. Fig. 3C shows that the surface hydrophobicity of ultrasonicated ZSP increased with the ultrasonic power increasing from 100 W to 400 W, reaching a maximum at 400 W. Similarly, the increased surface hydrophobicity of cactus (*Opuntia ficus-indica*) seed protein [13], *Cyperus esculentus* seed (tiger nut) protein [14] and wheat germ protein [2] after ultrasonic treatment was also reported. The above results could be due to the unfolding and the particle size reduction of the ZSP, exposing the hydrophobic regions inside the molecules to the surface [2,25]. On the other hand, the surface hydrophobicity of ZSP decreased with the ultrasonic power further increased, similar to the report of Yan et al. [8], which could be attributed to the reburial of some exposed hydrophobic groups would at excessive ultrasonic power.

3.4.4. Surface free SH content of ZSP

As an important active group in protein molecules, the free SH groups at the surface of proteins play a crucial role in influencing their emulsifying properties [13]. As present in Fig. 3D, the surface free SH of ZSP increased significantly ($P < 0.05$) after ultrasonic treatment at 100–400 W, reaching a maximum at 400 W. Considering the unchanged S-S bonds shown in the SDS-PAGE images, the increased surface free SH groups after ultrasonic treatment could be ascribed to the disruption of big protein aggregates into smaller particles and the structural unfolding of the protein molecules, surface exposing the buried SH groups inside them [2]. Similarly, the surface free SH content of walnut protein [34], wheat germ protein [2] and perilla protein isolate [3] was also increased after ultrasonic treatment. However, the surface free SH of ZSP decreased with the ultrasonic power further increased, indicating the reburial of some exposed SH groups at excessive ultrasonic power. The reduction of surface free SH groups of mussel actomyosin, mung bean protein has also been reported at excessive ultrasonic power [8,35].

3.5. EAI and ESI

EAI and ESI are commonly used to assess the emulsifying properties. Among them, EAI is the capacity of proteins to adsorb at the oil/water interface in the process of emulsion preparation, while ESI is the capacity of proteins to keep the emulsion stable [3,24]. As shown in Fig. 4A, native ZSP exhibited the lowest EAI and ESI of $42.64 \pm 1.52\ m^2/g$ and 38.26 ± 2.52 min, respectively.

The EAI of the ultrasonicated ZSP increased as the ultrasonic power increased from 100 W to 400 W, reaching the highest value ($98.44 \pm 1.86\ m^2/g$, about 2.31 folds of native ZSP) at 400 W. One possible explanation could be that the application of ultrasonic treatment led to the reduction in the particle diameter of ZSP (as depicted in Fig. 2C), which accelerated the diffusion rate of protein molecules at the oil/water interface and improved the EAI of ZSP. In addition, the increase in the surface hydrophobicity of ZSP (as shown in Fig. 3C) resulted in a more balanced ratio of hydrophilic and hydrophobic properties necessary for emulsification. This, in turn, facilitated the rapid absorption of the protein at the oil/water interface, leading to a reduction in interfacial tension, which further contributed to the improvement in EAI of ZSP [3,31]. A similar increase in EAI after ultrasonication has also been reported for perilla protein isolate and walnut protein isolate [3,11]. However, the higher ultrasonic power resulted in a reduction in EAI, which may be ascribed to the reduced interfacially adsorption rate caused by the increase in particle diameter and the decreased surface hydrophobicity of ZSP at the excessive ultrasonic power (Fig. 2C and Fig. 3C). A similar reduction in EAI has also been reported for *Moringa oleifera* seed protein and mussel actomyosin after ultrasonication at excessive power [8,17].

The change in ESI followed a similar trend to that of EAI, and the highest ESI value was also observed at of 400 W of ultrasound. One possible explanation could be that the application of ultrasonic treatment led to an increase in the α-helix content of ZSP (as shown in Table 1), which improved the structural compactness of ZSP and was helpful in maintaining the structural integrity of the proteins during emulsion formation and storage, thus increasing the EAI of ZSP [33]. In addition, the enhanced hydrophobic properties of ultrasonicated ZSP (as depicted in Fig. 3C) facilitated the interactions of the protein with the oil droplet through hydrophobic interactions, resulting in the formation of a more compact interfacial layer surrounding the oil droplets and ultimately improving the EAI of ZSP [3]. Furthermore, the increase in the surface free SH content (as shown in Fig. 3D) facilitates its exchange reaction with disulfide bonds, reinforcing the intermolecular interaction among protein molecules and facilitating their irreversible adsorption at the oil–water interface. This results in the formation of a highly viscoelastic membrane that effectively prevents protein aggregation, thereby contributing to an improved ESI of ZSP [13]. A similar result increase in ESI after ultrasonication has been reported for perilla protein isolate and walnut protein isolate [3,11]. Whereas, ESI decreased as the ultrasonic power was further increased, which might be mainly due to the re-folded tertiary structure of the ZSP (e.g., the decreased UV–vis absorbance, surface hydrophobicity, surface free SH content and increased intrinsic fluorescence spectra) at the excessive ultrasonic power, reducing the stability of the interfacial film between oil and water. Similar results were also observed for mussel sarcoplasmic protein, and mussel actomyosin after ultrasonic treatment at excessive power [8,22].

3.6. Interfacial protein adsorption of emulsions

The content of protein interfacially adsorbed is critical for emulsion stability [3]. As depicted in Fig. 4B, much more interfacial adsorbed

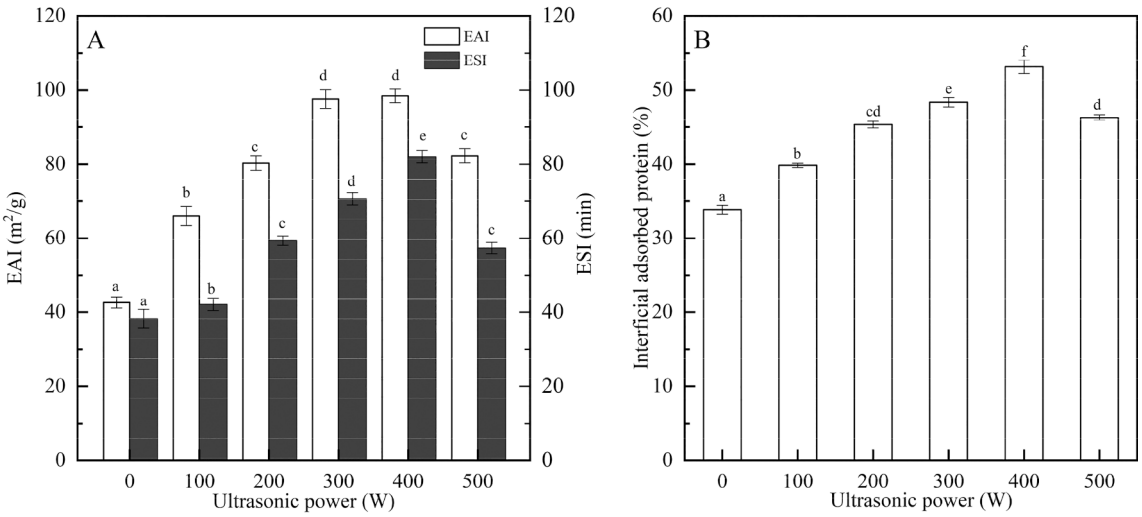

Fig. 4. EAI and ESI (A) and Interfacial protein adsorption (B) of native and ultrasonicated ZSP. Different lowercase letters in the column diagram suggest significant differences ($P < 0.05$).

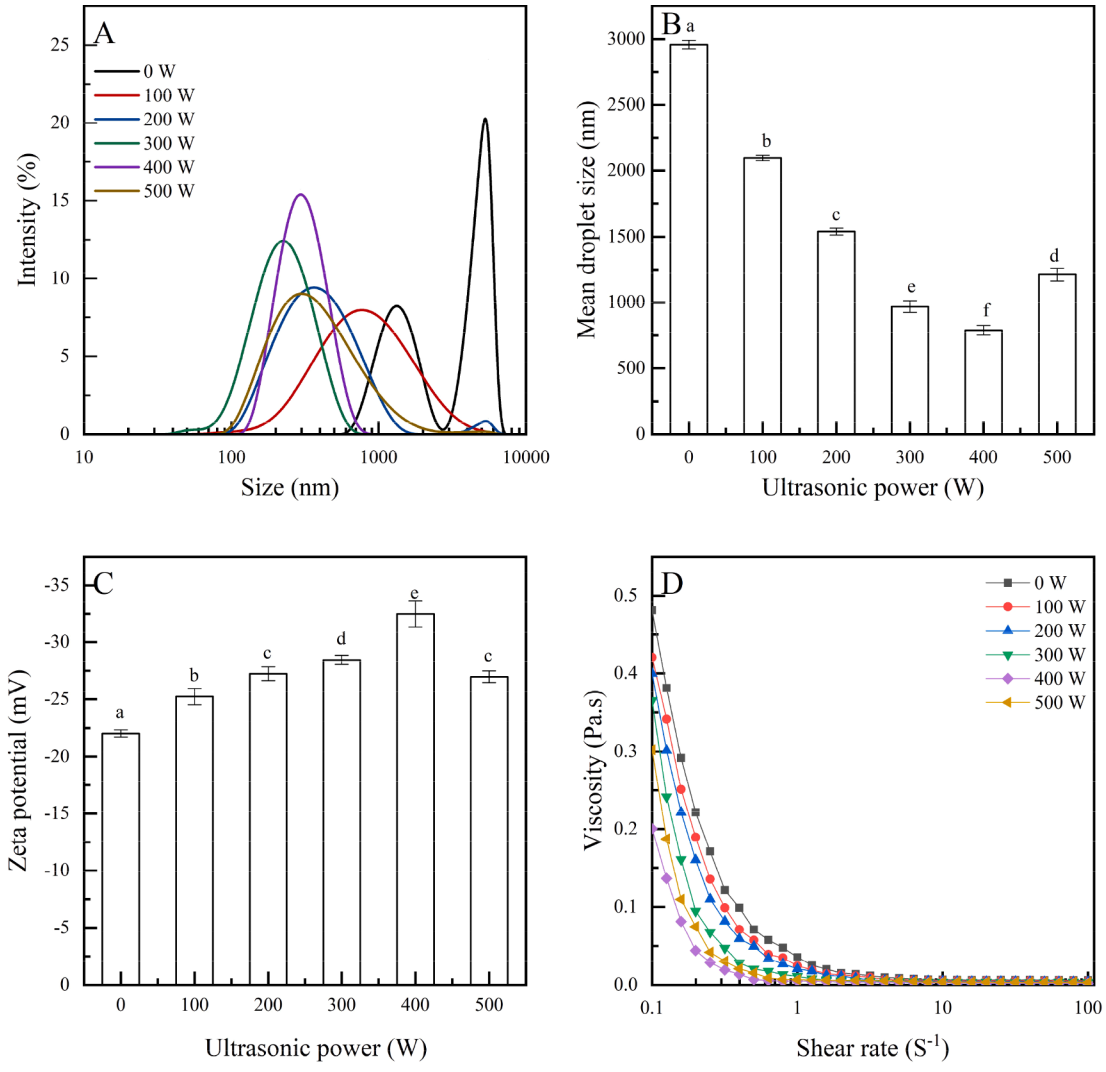

Fig. 5. The microstructure of emulsions of native or ultrasonicated ZSP. The long and short red bars in the figures represent 10 μm and 1 μm, respectively.

protein was observed in the emulsion stabilized by ultrasonically modified ZSP than in the emulsion stabilized by native ZSP. It increased significantly ($p < 0.05$) as the ultrasonic power raised from 100 W to 400 W, reaching the highest value (53.14 ± 0.92 %, about 1.57 folds of native ZSP) at 400 W. This result could be ascribed to a decline in particle size and an increase in the surface hydrophobicity of the proteins led by the ultrasonic treatment, which enhanced their mobilization and promoted their interfacially adsorption [24,27]. Similarly, the emulsions prepared from ultrasonicated perilla protein isolate [3] and mussel actomyosin [8] also exhibited a significantly ($P < 0.05$) higher interfacial adsorbed protein than those stabilized by native proteins. However, the content of interfacially adsorbed protein reduced with further raise in ultrasonic power, consistent with the report of Yan et al. [8], which may be due to the increased particle size and the decreased surface hydrophobicity of the proteins, slowing down their interfacially adsorption rate.

3.7. The microstructures of the emulsions

Fig. 5 exhibited the microstructures of the emulsions under a light microscope. Large emulsion droplets with uneven droplet distribution were observed in the emulsion of native ZSP. In contrast, the emulsion of ultrasonicated ZSP exhibited the smaller droplets with the more uniform distribution. In particular, the emulsion of ZSP ultrasonicated at 400 W showed the smallest droplet and the most uniform distribution. This might be ascribed to the improved interfacial adsorption capacity of proteins, which decreases the surface interfacial tension and inhibits the aggregation of emulsion droplets [2].

3.8. The droplet size of emulsion

Emulsion droplet size is critical to emulsion stability and small droplet size is beneficial to reduce the van der Waals forces between droplets and prevent the emulsion from aggregating and gravitationally separating, thereby improving emulsion stability [11]. Fig. 6A exhibits the droplet size dispersion of freshly prepared emulsion, of native or ultrasonicated ZSP. The droplet size dispersion of the native ZSP-stabilized emulsion was relatively broad, ranging from about 700 nm to 5560 nm, and showed two peaks around 1280 nm and 4800 nm. The dispersion curves of droplet size in the emulsion exhibited a leftward shift and narrowing when ultrasonicated ZSP samples were used as emulsifier. As depicted in Fig. 6B, the mean droplet size of the emulsion prepared by ultrasonicated ZSP decreased as the ultrasonic power raised from 100 W to 400 W, reaching the lowest value (789.60 ± 36.53 nm, about 26.69 % of native ZSP) at 400 W. This can be attributed to that the surface exposure of hydrophobic groups inside protein molecules and the structural unfolding of the protein, leading to a large number of proteins interfacially adsorbed (Fig. 4B). Similarly, emulsions prepared from ultrasonicated mussel actomyosin [8] and ultrasonicated perilla protein isolate [3] also exhibited a smaller droplet size than those prepared from native proteins. However, the mean droplet size of the ultrasonicated ZSP-stabilized emulsion increased as the ultrasonic power was further raised. The changes in emulsion droplet size were similar to those of EAI, ESI, interfacially adsorbed protein and the emulsion microstructures (Fig. 4A and Fig. 4B), which could be due to the reduced interfacial adsorption capacity of the protein induced by the protein reaggregation at excessive ultrasonic power [8]. Similar results have been observed for other ultrasonicated proteins (e.g., mussel sarcoplasmic protein, *Moringa oleifera* seed protein and mussel actomyosin) [8,17,22].

Zeta-potential is also related to emulsion stability, and the emulsion with the higher zeta-potential has a lower tendency to aggregate due to the stronger electrostatic repulsion between droplets [11]. Fig. 6C shows that all the fresh emulsions displayed negative zeta-potential in distilled water at neutral pH. In addition, the fresh emulsion stabilized by ultrasonicated ZSP exhibited much higher negative zeta-potential than that by native ZSP. The fresh emulsion with the highest value of negative zeta-potential (−32.50 ± 1.15 mV, about 1.48 folds of native ZSP) was obtained when ZSP was treated at 400 W and used as an emulsifier, which can be attributed to the slightly higher zeta-potential of ultrasonicated ZSP, as well as the higher amount of interfacial adsorbed protein in the emulsion [3]. Similarly, the emulsions prepared from ultrasonicated perilla protein isolate [3] and ultrasonicated walnut protein [11] also exhibited a higher negative zeta-potential than the control.

3.9. Static rheological properties of emulsions

The viscosity patterns of emulsions prepared from native/ultrasonicated ZSP are depicted in Fig. 6D. The decrease in viscosity with increasing shear rate was observed, indicating the shear-thinning (pseudoplastic) properties of the emulsions. Compared to native ZSP, the viscosity of the emulsions prepared from ultrasonicated ZSP decreased as the ultrasonic power raised from 100 W to 400 W and then increased with further raise in ultrasonic power. According to Zou et al. [22], the flocculated emulsion has the higher viscosity than the non-

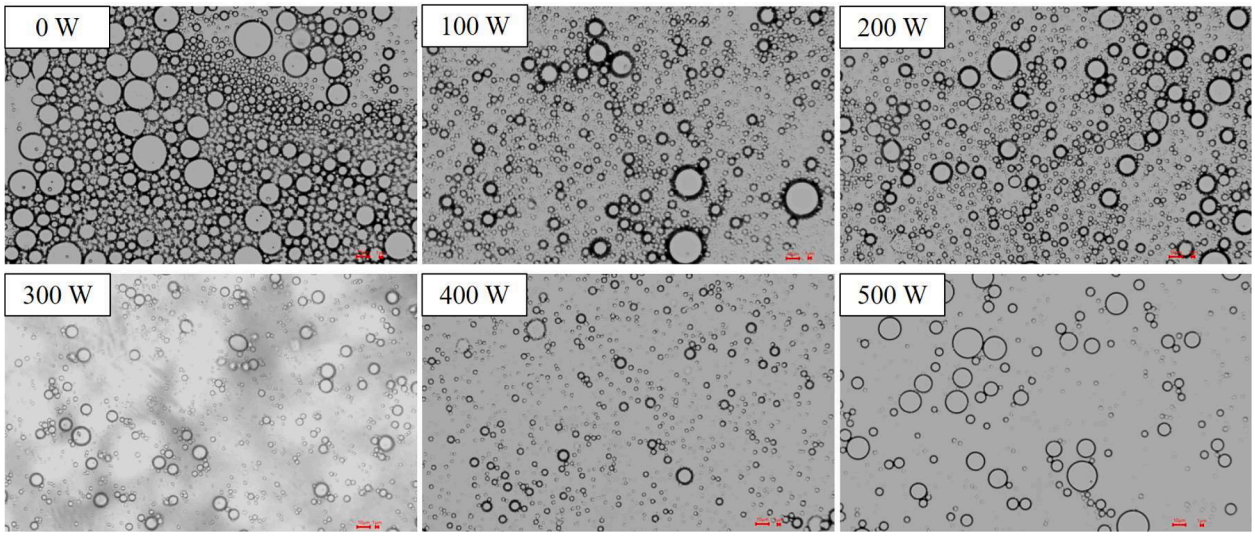

Fig. 6. The droplet size dispersion (A), mean droplet size (B) and zeta-potential (C) and static rheological properties (D) of emulsion stabilized by native and ultrasonicated ZSP. Different lowercase letters in the column diagram suggest significant differences ($P < 0.05$).

flocculated sample at the same concentration. Thus, the smaller oil droplets in the emulsions prepared from ultrasonicated ZSP contributed to their reduced viscosity. In addition, the decreased viscosity may also be related to the particle size reduction of ZSP caused by the cacitation effects of ultrasonic treatment [8]. A similar variation tendency was observed in oil/water emulsions prepared from ultrasonicated mussel sarcoplasmic protein and ultrasonicated mussel actomyosin [8,22].

3.10. The stability of emulsions against environmental stresses

Heat stability

In general, the emulsion experienced an increase in particle size during heat treatment, which may be due to the aggregation of the protein interfacially adsorbed and the accumulation of the protein dispersed in the water phase [36]. As depicted in Table 2, the droplet size of the emulsion prepared from ultrasonicated ZSP was much smaller than that of native ZSP after heating at 70–90 °C for 30 min, indicating their better thermal stability. In addition, the droplet size of the ultrasonicated ZSP-stabilized emulsion after heat treatment decreased as the ultrasonic power raised from 100 W to 400 W and then increased with further raise in ultrasonic power. The increased thermal stability of the ultrasonicated ZSP-stabilized emulsion is probably due to the decreased droplet size of the emulsion and the increased amount of proteins interfacially adsorbed, creating a more durable and thicker interfacial film, which aids in preserving the stability of the emulsion when subjected to heat treatment [37]. Similarly, the increased thermal stability was also observed in emulsions stabilized with ultrasonicated sodium caseinate [38].

Table 2
The stability of emulsions prepared from native and ultrasonicated ZSP against environmental stresses (thermal, salt ion, and pH).

Ultrasonic power (W)	Temperature			
	25	70	80	90
0	2958.15 ± 32.13[a]	5372.29 ± 38.64[b]	7608.94 ± 41.25[c]	9145.60 ± 49.73[d]
100	2095.34 ± 20.36[a]	3501.68 ± 34.52[b]	5146.98 ± 29.67[c]	7217.26 ± 42.58[d]
200	1541.03 ± 26.35[a]	2379.65 ± 28.89[b]	3168.41 ± 39.47[c]	4869.58 ± 32.46[d]
300	968.60 ± 44.51[a]	1487.46 ± 25.84[b]	1979.56 ± 29.75[c]	2972.29 ± 38.85[d]
400	789.60 ± 36.53[a]	1167.42 ± 21.89[b]	1601.72 ± 32.16[c]	2328.47 ± 25.61[d]
500	1212.66 ± 48.70[a]	1835.41 ± 31.68[b]	2526.83 ± 35.17[c]	3894.26 ± 41.32[d]
	NaCl concentration (mM)			
	0	100	200	300
0	2958.15 ± 32.13[a]	4124.96 ± 45.67[b]	5495.66 ± 42.81[c]	5644.14 ± 35.78[d]
100	2095.34 ± 20.36[a]	3174.30 ± 23.21[b]	4326.04 ± 31.35[c]	4506.29 ± 36.45[d]
200	1541.03 ± 26.35[a]	2505.91 ± 27.76[b]	3415.61 ± 38.46[c]	3517.88 ± 23.21[d]
300	968.60 ± 44.51[a]	1588.19 ± 38.23[b]	2209.21 ± 36.53[c]	2337.05 ± 36.53[d]
400	789.60 ± 36.53[a]	1141.90 ± 31.67[b]	1554.62 ± 41.58[c]	1685.33 ± 37.46[d]
500	1212.66 ± 48.70[a]	2013.78 ± 35.42[b]	2772.64 ± 29.76[c]	2885.25 ± 48.70[d]
	pH			
	3.0	5.0	7.0	9.0
0	5392.20 ± 41.27[b]	7596.68 ± 39.86[c]	2958.15 ± 32.13[a]	2902.68 ± 38.25[a]
100	4594.45 ± 37.63[b]	6872.61 ± 29.72[c]	2095.34 ± 20.36[a]	2043.36 ± 32.46[a]
200	4196.42 ± 27.18[b]	6036.43 ± 41.15[c]	1541.03 ± 26.35[a]	1486.18 ± 31.65[a]
300	3569.13 ± 32.26[b]	4859.98 ± 25.48[c]	968.60 ± 44.51[a]	909.23 ± 28.49[a]
400	2379.15 ± 24.35[b]	3660.81 ± 32.54[c]	789.60 ± 36.53[a]	723.80 ± 34.27[a]
500	3864.51 ± 29.67[b]	5214.23 ± 36.79[c]	1212.66 ± 48.70[a]	1168.41 ± 44.35[a]

[a] Different lowercase letters in each column suggest significant differences ($p < 0.05$).

3.10.1. Salt ion stability

The stability of emulsion against salt ions is a critical parameter in evaluating its application. The presence of NaCl facilitated the flocculation and aggregation of emulsion by altering its surface charge [39]. According to Table 2, it was observed that there was a notable increase in droplet size for all emulsions as the ionic strength increased. However, the emulsion stabilized by ultrasonicated ZSP at varying salt concentrations exhibited comparatively smaller droplet sizes compared to those of native ZSP. The smallest droplet size at different salt concentrations was observed in the emulsion stabilized by 400 W ultrasonicated ZSP, likely due to its highest zeta-potential (Fig. 6C), which mitigates the destabilizing effect of different salt concentrations. Similarly, the increased ionic stability was also observed in emulsions stabilized with ultrasonicated egg white protein peptides [40].

3.10.2. pH stability

During processing, storage and transportation, food products are always exposed to varying pH levels. Hence, it is imperative to examine the durability of emulsions across various pH values. From Table 2, it can be seen that the droplet size of all emulsions increased significantly at pH 3 and pH 5 and decreased slightly at pH 9.0. The increase in droplet size of emulsions at pH 3 and pH 5 can be attributed to the fact that the pH 3 and pH 5 were in proximity to the isoelectric point (pI) of the ZSP, resulting in insufficient electrostatic repulsion among the emulsion droplets and subsequently polymerization of these droplets [41]. In addition, the droplet size of the emulsion prepared from ultrasonicated ZSP at different pH was smaller than that of native ZSP. The smallest droplet size at different pH was observed in the emulsion stabilized by 400 W ultrasonicated ZSP, likely due to its highest zeta-potential (Fig. 6C), which mitigates the destabilizing effect of the pH values close to the PI of the ZSP.

3.11. Creaming stability

Creaming is the upward movement of the larger oil droplets and the formation of an oily layer at the top of the emulsion due to differences in density. The lower creaming index values of the emulsion represented the higher creaming stability [24]. As depicted in Fig. 7A, the creaming index of ultrasonicated ZSP-stabilized emulsions was much lower than that of the native ZSP, indicating their better creaming stability. In addition, the decrease in creaming index of the ultrasonicated ZSP-stabilized emulsion was observed as the ultrasonic power increased from 100 W to 400 W, reaching the lowest creaming index at 400 W, and then increasing with the ultrasonic power further increased. The increased creaming stability of the ultrasonicated ZSP-stabilized emulsion could be attributed to their reduced droplet size [3]. Besides that, the increased amount of proteins interfacially adsorbed would also increase the electrostatic repulsion among emulsion droplets and improve the viscoelasticity of the interfacial film, thus increasing creaming stability [34]. Similarly, an increased creaming stability has been also observed in emulsions stabilized with ultrasonicated mussel actomyosin [8], ultrasonicated perilla protein isolate [3], ultrasonicated cod protein [24] and others.

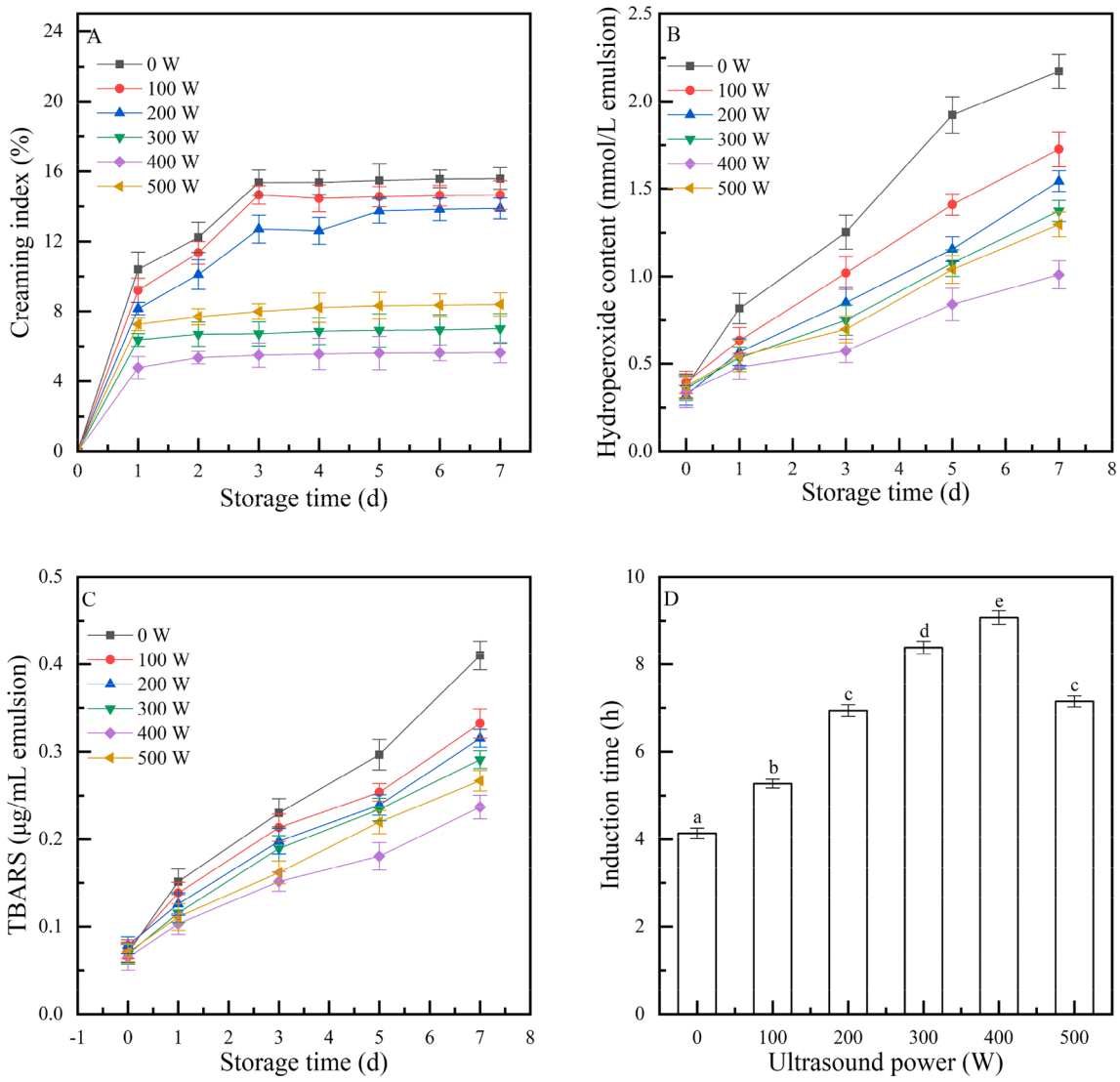

Fig. 7. The creaming index (A), hydroperoxides (B), TBARS (C) and rancimat induction time (D) of the emulsion stabilized by native and ultrasonicated ZSP during storage. Different lowercase letters in the column diagram suggest significant differences ($P < 0.05$).

3.12. Lipid oxidative stability in O/W emulsion

Emulsions with a high content of polyunsaturated fatty acids are prone to undergoing oxidation. As shown in Fig. 7B and Fig. 7C, the initial content of hydroperoxides and TBARS in all emulsions was about 0.3 mmol/L and about 0.07 μg/mL, respectively, which increased continuously in all emulsions during storage. The emulsion stabilized by native ZSP exhibits the fastest increase, whereas the increase in hydroperoxides and TBARS content was relatively slow in the emulsions prepared from ultrasonicated ZSP, especially in the emulsion prepared from ZSP ultrasonicated at 400 W. Besides that, the rancimat induction time of the emulsion prepared from ultrasonicated ZSP (400 W) was 9.17 ± 0.06 h, much longer than that of the emulsion stabilized by native ZSP (6.73 ± 0.11 h) (Fig. 7D).

The improved oxidative stability of the emulsion prepared from ultrasonicated protein could be due to the viscoelastic and thick interfacial membrane formed by the ultrasonicated proteins, which may form a steric hindrance between the aqueous and lipid phases, thereby preventing the lipids from oxidation to some extent [12,24,27]. In addition, interfacial adsorbed proteins could retard lipid oxidation by being oxidized or by binding to the lipid oxidation products [11]. Similarly, the increased oxidative stability was also observed in the emulsion stabilized by ultrasonicated walnut protein [11] and ultrasonicated *Neosalanx taihuensis* myofibrillar protein [12].

A schematic (Fig. 8) was drawn to explain the possible mechanism for the improvement of the emulsifying properties of ZSP through ultrasonic treatment. Native ZSP cannot rapidly adsorb at the water/oil interface and form a thick and stable interfacial film around oil droplets, mainly due to its larger size and lower surface hydrophobicity. Ultrasonic treatment dissociates and unfolds the ZSP, resulting in a decrease in particle size and an increase in the exposure of active groups (e.g., hydrophobic groups and hydrophobic groups), resulting in more protein interfacially adsorbed and a smaller size of emulsion droplet, increasing the thickness and stability of the interfacial film through the interaction between active groups, preventing the emulsion from coalescing and flocculating, thereby improving the stability against environmental stress (temperature, salt concentration, pH), creaming and oxidation of the prepared emulsions.

4. Conclusions

This study demonstrated that the ultrasonic modification resulted in a substantial reduction in particle size, concurrently inducing the conformational alterations and structure unfolding in ZSP molecules.

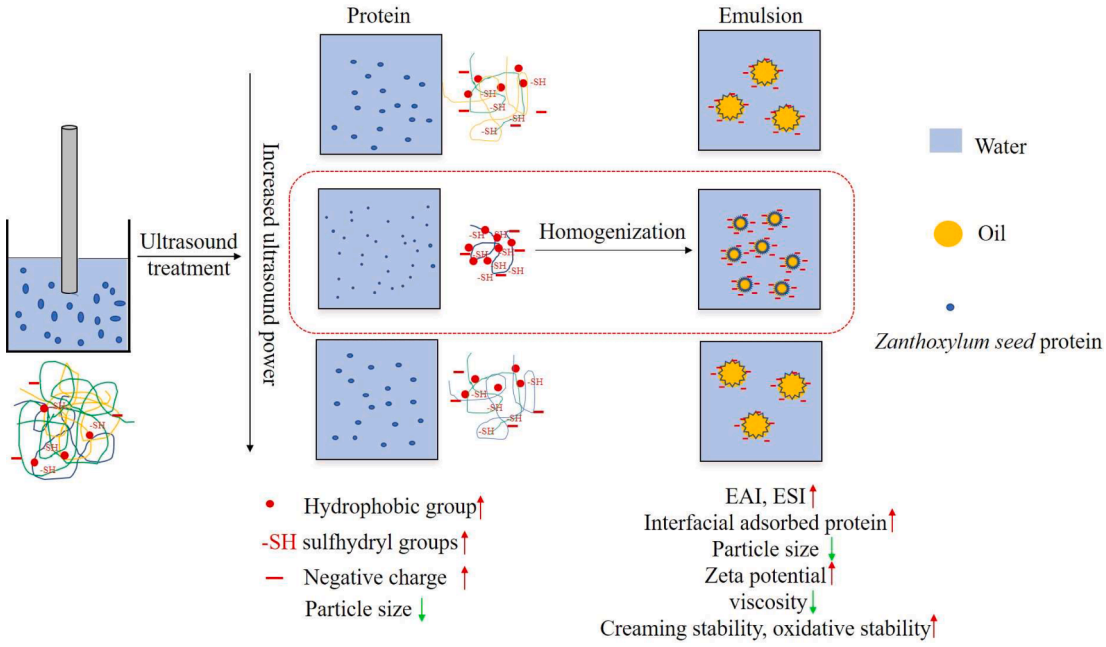

Fig. 8. Schematic of the possible mechanism for the improvement of the emulsifying properties of ZSP by the ultrasonic treatment.

Consequently, this led to an augmentation in α-helix, ultraviolet–visible absorbance, surface hydrophobicity and the content of free sulfhydryl groups. These alterations ultimately enhanced the emulsifying properties of ZSP. Moreover, it was confirmed that ultrasonically treated ZSP yielded an emulsion with a smaller and more consistent droplet size distribution, higher amount of interfacial protein adsorption, higher stability against environmental stresses (temperature, salt concentration and pH), higher creaming stability and higher oxidative stability. These results suggested that ultrasonic modification of ZSP can improve its emulsion stability, thereby underscoring its potential as a stabilizer for developing emulsion-based products.

CRediT authorship contribution statement

Qingqing Liu: Conceptualization, Methodology, Formal analysis, Investigation, Writing – original draft, Writing – review & editing. **Yanting Liu:** Methodology, Investigation, Formal analysis, Writing – original draft. **He Huang:** Investigation. **Mingming Xiong:** Investigation. **Yunting Yang:** Investigation. **Chutian Lin:** Investigation. **Feng Yang:** Investigation. **Yisha Xie:** Writing – review & editing. **Yongjun Yuan:** Project administration, Supervision, Validation.

Declaration of Competing Interest

The authors declare that they have no known competing financial interests or personal relationships that could have appeared to influence the work reported in this paper.

Acknowledgements

This work was supported by the Key Natural Science Foundation of Xihua University (Z17126).

References

[1] N. Thalia Flores-Jimenez, J. Armando Ulloa, J. Esmeralda Urias-Silvas, J. Carmen Ramirez-Ramirez, P. Ulises Bautista-Rosales, R. Gutierrez-Leyva, Influence of high-intensity ultrasound on physicochemical and functional properties of a *guamuchil Pithecellobium dulce* (Roxb.) seed protein isolate, Ultrason. Sonochem. 84 (2022), 105976.

[2] X. Li, T. Luo, L. Wang, H. Song, F. Wang, Z. Weng, J. Zhou, X. Xiang, L. Xiong, X. Shen, Emulsifying properties of wheat germ protein: Effect of different ultrasonic treatment, Ultrason. Sonochem. 98 (2023) 106479.

[3] Q. Zhao, T. Xie, X. Hong, Y. Zhou, L. Fan, Y. Liu, J. Li, Modification of functional properties of perilla protein isolate by high-intensity ultrasonic treatment and the stability of o/w emulsion, Food Chem. 368 (2022), 130848.

[4] P. Meinlschmidt, U. Schweiggert-Weisz, V. Brode, P. Eisner, Enzyme assisted degradation of potential soy protein allergens with special emphasis on the technofunctionality and the avoidance of a bitter taste formation, LWT-, Food Sci. Technol. 68 (2016) 707–716.

[5] H. Wang, Y. Chen, Y. Hua, X. Kong, C. Zhang, Effects of phytase-assisted processing method on physicochemical and functional properties of soy protein isolate, J. Agric. Food Chem. 62 (45) (2014) 10989–10997.

[6] Q. Luo, X. Li, Z. Zhang, A. Chen, S. Li, G. Shen, M. Li, X. Liu, X. Yin, L. Cheng, X. Yang, C. Jiang, J. Li, X. Hou, Extraction of Zanthoxylum seed protein and identification of its simulated digestion products, LWT- Food Sci. Technol. 161 (2022), 113412.

[7] Guo, J., X. Xiao, J. Miao, B. Tian, J. Zhao, and Y. Lan, Design and experiment of a visual detection system for *Zanthoxylum*-harvesting robot based on improved YOLOv5 Model, Agriculture. 13(4) (2023) 821.

[8] H. Yan, H. Zou, S. Li, S. Sun, Q. Xu, C. Yu, Modification of functional properties of mussel actomyosin by ultrasound treatment and the appplication at O/W emulsion, LWT- Food Sci. Technol. 170 (2022), 114086.

[9] W. Chen, H. Ma, Y.Y. Wang, Recent advances in modified food proteins by high intensity ultrasound for enhancing functionality: Potential mechanisms, combination with other methods, equipment innovations and future directions, Ultrason. Sonochem. 85 (2022), 105993.

[10] D. Xu, C. Li, Z. Zhuo, M. Ye, B. Fu, B. Pu, Physicochemical and Emulsifying Properties of Protein Extracted from *Zanthoxylum armatum* Seed Kernel, Iran J. Sci. Technol. Trans Sci. 44 (1) (2019) 65–73.

[11] L.S. Shi, X.Y. Yang, T. Gong, C.Y. Hu, Y.H. Shen, Y.H. Meng, Ultrasonic treatment improves physical and oxidative stabilities of walnut protein isolate-based emulsion by changing protein structure, LWT- Food Sci. Technol. 173 (2023), 114269.

[12] X.H. Deng, X.X. Ni, J.H. Han, W.H. Yao, Y.J. Fang, Q. Zhu, M.F. Xu, High-intensity ultrasound modified the functional properties of *Neosalanx taihuensis* myofibrillar protein and improved its emulsion stability, Ultrason. Sonochem. 97 (2023), 106458.

[13] X. Li, B. Qi, S. Zhang, Y. Li, Effects of ultrasonic treatment on the structural and functional properties of cactus (*Opuntia ficus-indica*) seed protein, Ultrason. Sonochem. 97 (2023), 106465.

[14] Q. Cui, L. Wang, G. Wang, A. Zhang, X. Wang, L. Jiang, Ultrasonication effects on physicochemical and emulsifying properties of *Cyperus esculentus* seed (tiger nut) proteins, LWT- Food Sci. Technol. 142 (2021), 110979.

[15] A. Vera, M. Valenzuela, M. Yazdani-Pedram, C. Tapia, L. Abugoch, Conformational and physicochemical properties of quinoa proteins affected by different conditions of high-intensity ultrasound treatments, Ultrason. Sonochem. 51 (2019) 186–196.

[16] Z. Zhang, J.M. Regenstein, P. Zhou, Y. Yang, Effects of high intensity ultrasound modification on physicochemical property and water in myofibrillar protein gel, Ultrason. Sonochem. 34 (2017) 960–967.

[17] S.Q. Tang, Q.H. Du, Z. Fu, Ultrasonic treatment on physicochemical properties of water-soluble protein from Moringa oleifera seed, Ultrason. Sonochem. 71 (2021), 105357.
[18] Y. Zou, H. Shi, X. Chen, P. Xu, D. Jiang, W. Xu, D. Wang, Modifying the structure, emulsifying and rheological properties of water-soluble protein from chicken liver by low-frequency ultrasound treatment, Int. J. Biol. Macromol. 139 (2019) 810–817.
[19] W. Xiong, Y. Wang, C. Zhang, J. Wan, B.R. Shah, Y. Pei, B. Zhou, J. Li, B. Li, High intensity ultrasound modified ovalbumin: Structure, interface and gelation properties, Ultrason. Sonochem. 31 (2016) 302–309.
[20] J. Chen, X. Li, C. Cao, B. Kong, H. Wang, H. Zhang, Q. Liu, Effects of different pH conditions on interfacial composition and protein-lipid co-oxidation of whey protein isolate-stabilised O/W emulsions, Food Hydrocoll. 131 (2022), 107752.
[21] L. Sha, A.O. Koosis, Q. Wang, A.D. True, Y.L. Xiong, Interfacial dilatational and emulsifying properties of ultrasound-treated pea protein, Food Chem. 350 (2021), 129271.
[22] H. Zou, N. Zhao, S. Sun, X. Dong, C. Yu, High-intensity ultrasonication treatment improved physicochemical and functional properties of mussel sarcoplasmic proteins and enhanced the stability of oil-in-water emulsion, Colloids Surf. Physicochem. Eng. Aspects. 589 (2020), 124463.
[23] B. Rajasekaran, A. Singh, A. Ponnusamy, U. Patil, B. Zhang, H. Hong, S. Benjakul, Ultrasound treated fish myofibrillar protein: Physicochemical properties and its stabilizing effect on shrimp oil-in-water emulsion, Ultrason. Sonochem. 98 (2023), 106513.
[24] K. Li, L. Fu, Y.-Y. Zhao, S.-W. Xue, P. Wang, X.-L. Xu, Y.-H. Bai, Use of high-intensity ultrasound to improve emulsifying properties of chicken myofibrillar protein and enhance the rheological properties and stability of the emulsion, Food Hydrocoll. 98 (2020), 105275.
[25] D. Wu, C. Wu, W. Ma, Z. Wang, C. Yu, M. Du, Effects of ultrasound treatment on the physicochemical and emulsifying properties of proteins from scallops (*Chlamys farreri*), Food Hydrocoll. 89 (2019) 707–714.
[26] X. Lu, H. Su, J. Guo, J. Tu, Y. Lei, S. Zeng, Y. Chen, S. Miao, B. Zheng, Rheological properties and structural features of coconut milk emulsions stabilized with maize kernels and starch, Food Hydrocoll. 96 (2019) 385–395.
[27] W. Ma, J. Wang, X. Xu, L. Qin, C. Wu, M. Du, Ultrasound treatment improved the physicochemical characteristics of cod protein and enhanced the stability of oil-in-water emulsion, Food Res. Int. 121 (2019) 247–256.
[28] J. Yi, J. Ning, Z. Zhu, L. Cui, E.A. Decker, D.J. McClements, Impact of interfacial composition on co-oxidation of lipids and proteins in oil-in-water emulsions: Competitive displacement of casein by surfactants, Food Hydrocoll. 87 (2019) 20–28.
[29] Fregapane, G., C. Cabezas Fernandez, and M.D. Salvador, Emulsion and microemulsion systems to improve functional edible oils enriched with walnut and pistachio phenolic extracts, Foods. 11(9) (2022) 1210.
[30] R. Mozafarpour, A. Koocheki, T. Nicolai, Modification of grass pea protein isolate (*Lathyrus sativus L.*) using high intensity ultrasound treatment: Structure and functional properties, Food Res. Int. 158 (2022), 111520.
[31] D. Huang, W. Li, G. Li, W. Zhang, H. Chen, Y. Jiang, D. Li, Effect of high-intensity ultrasound on the physicochemical properties of Tenebrio Molitor Protein, Food Hydrocoll. 134 (2023), 108056.
[32] F. Alavi, L. Chen, Z. Emam-Djomeh, Effect of ultrasound-assisted alkaline treatment on functional property modifications of faba bean protein, Food Chem. 354 (2021), 129494.
[33] Z. Zuo, Z. Geng, X. Zhang, T. Ma, H. Liu, L. Wang, Ultrasonic treatment influences the compactness of quinoa protein microstructure and improves the structural integrity of quinoa protein at the interfaces of high internal phase emulsion, Food Res. Int. 168 (2023), 112713.
[34] Z. Zhu, W. Zhu, J. Yi, N. Liu, Y. Cao, J. Lu, E.A. Decker, D.J. McClements, Effects of sonication on the physicochemical and functional properties of walnut protein isolate, Food Res. Int. 106 (2018) 853–861.
[35] R.-X. Wang, Y.-Q. Li, G.-J. Sun, C.-Y. Wang, Y. Liang, D.-L. Hua, L. Chen, H.-Z. Mo, The improvement and mechanism of gelation properties of mung bean protein treated by ultrasound, LWT- Food Sci. Technol. 182 (2023), 114811.
[36] S. Yang, Z. Lian, M. Wang, P. Liao, H. Wu, J. Cao, X. Tong, T. Tian, H. Wang, L. Jiang, Molecular structural modification of beta-conglycinin using pH-shifting with ultrasound to improve emulsifying properties and stability, Ultrason. Sonochem. 90 (2022), 106186.
[37] N. Wang, Z. Ma, L. Ma, Y.e. Zhang, K. Zhang, Q. Ban, X. Wang, Synergistic modification of structural and functional characteristics of whey protein isolate by soybean isoflavones non-covalent binding and succinylation treatment: A focus on emulsion stability, Food Hydrocoll. 144 (2023) 108994.
[38] X. He, S. Jia, J. Wan, Y. Li, Y. Zhang, H. Zhu, K. Li, Effects of high-intensity ultrasound treatments on the physicochemical and structural characteristics of sodium caseinate (SC) and the stability of sc-coated oil-in-water (O/W) emulsions, Foods. 11 (18) (2022) 2817.
[39] N. Wang, R. Wang, K. Xing, Z. Huang, W. Elfalleh, H. Zhang, D. Yu, Microfluidization of soybean protein isolate-tannic acid complex stabilized emulsions: Characterization of emulsion properties, stability and in vitro digestion properties, Food Chem. 430 (2023), 137065.
[40] M. Ai, Z. Zhang, H. Fan, Y. Cao, A. Jiang, High-intensity ultrasound together with heat treatment improves the oil-in-water emulsion stability of egg white protein peptides, Food Hydrocoll. 111 (2021), 106256.
[41] Y. Chen, L. Li, X. Zhao, X. Zeng, X. Xu, How environmental stresses affect the physical stability of oil in water emulsion prepared using pH-shifted myofibrillar protein? LWT- Food Sci. Technol. 186 (2023) 115200.
[42] J. Zhang, Q. Liu, Q. Chen, F. Sun, H. Liu, B. Kong, Synergistic modification of pea protein structure using high-intensity ultrasound and pH-shifting technology to improve solubility and emulsification, Ultrason. Sonochem. 88 (2022) 106099.